

2013

A Review of Luminescent Anionic Nano System: d^{10} Metallo cyanide Excimers and Exciplexes in Alkali Halide Hosts

Xiabo Li

Howard H. Patterson
University of Rhode Island

Creative Commons License

[Creative Commons License](#)

This work is licensed under a [Creative Commons Attribution-Share Alike 3.0 License](#).

Follow this and additional works at: https://digitalcommons.uri.edu/chm_facpubs

Citation/Publisher Attribution

Li, X., & Patterson, H. (2013). A Review of Luminescent Anionic Nano System: d^{10} Metallo cyanide Excimers and Exciplexes in Alkali Halide Hosts. *Materials*, 6(7), 2595–2611. doi:10.3390/ma6072595
Available at: <https://doi.org/10.3390/ma6072595>

This Article is brought to you for free and open access by the Chemistry at DigitalCommons@URI. It has been accepted for inclusion in Chemistry Faculty Publications by an authorized administrator of DigitalCommons@URI. For more information, please contact digitalcommons@etal.uri.edu.

Review

A Review of Luminescent Anionic Nano System: d^{10} Metallo cyanide Excimers and Exciplexes in Alkali Halide Hosts

Xiaobo Li ^{1,2} and Howard H. Patterson ^{1,*}

¹ Department of Chemistry, University of Maine, Orono, ME 04469, USA;

E-Mail: xli@chm.uri.edu

² Department of Chemistry, University of Rhode Island, Kingston, RI 02881, USA

* Author to whom correspondence should be addressed; E-Mail: howardp@maine.edu;

Tel.: +1-207-581-1178; Fax: +1-207-581-1191.

Received: 2 May 2013; in revised form: 8 June 2013 / Accepted: 18 June 2013 /

Published: 25 June 2013

Abstract: Dicyanoaurate, dicyanoargentate, and dicyanocuprate ions in solution and doped in different alkali halide hosts exhibit interesting photophysical and photochemical behavior, such as multiple emission bands, exciplex tuning, optical memory, and thermochromism. This is attributed to the formation of different sizes of nanoclusters in solution and in doped hosts. A series of spectroscopic methods (luminescence, UV-reflectance, IR, and Raman) as well as theoretical calculations have confirmed the existence of excimers and exciplexes. This leads to the tunability of these nano systems over a wide wavelength interval. The population of these nanoclusters varies with temperature and external laser irradiation, which explains the thermochromism and optical memory. DFT calculations indicate an MLCT transition for each nanocluster and the emission energy decreases with increasing cluster size. This is in agreement with the relatively long life-time for the emission peaks and the multiple emission peaks dependence upon cluster concentration.

Keywords: excimers; exciplexes; d^{10} cyanide systems; alkali halide nano systems; dimmers; trimers

1. Introduction

The term “excimer” was first introduced in 1960 by Stevens and Hutton when studying pyrene luminescence [1]. They defined excimer as a dimer associated in the electronic excited state and dissociated in its ground state, which is different from a stable dimer. Actually, the first excimer can be dated back to 1927, when Lord Rayleigh observed the ultraviolet emission spectrum of high-pressure mercury vapor [2]. Nobel gases, such as Helium, Neon, Argon, and Krypton also form excimers to give intense emission spectra in the vacuum ultraviolet region [3,4]. Excimers are also common in liquid and solid phases, especially for aromatic compounds. As early as the 1950s, Förster and Kasper observed that the pyrene solution fluorescence depended on the concentration [5,6]. Since then, more and more organic compounds have been found to form excimers: benzene, naphthalene, 1,2-benzanthracene, and perylene, just to name a few [7–11].

For inorganic excimers, a matrix isolation study has been carried out for alkali metals, alkaline earth metals and group VIIB metals with absorption and luminescence spectra [12]. Platinum complexes have been reported to form different excimers in aqueous solution, such as $[\text{PtII}(4,7\text{-diphenyl-1,10-phenanthroline})(\text{CN})_2]$, $[\text{Pt}_2(\text{P}_2\text{O}_5\text{H}_2)_4^{2-}\text{TI}]$, and $[\text{Pt}_2(\text{P}_2\text{O}_5\text{H}_2)_4^{2-}\text{Au}(\text{CN})_2^-]$ [13–15]. In aqueous solution, the formation of excimers is affected by the concentration of monomers; as the concentration increases, the emission peak intensity corresponding to the excimer is enhanced. Closed-shell heavy metals used to be considered as repelling each other due to the fully occupied valence orbitals. However, in the study of inorganic and organometallic compounds, experimental results have presented evidence of interaction between closed-shell metals [16–25]. The strength of these bonds is weaker than ionic (700–4000 kJ/mol) and covalent bonds (200–1000 kJ/mol) but stronger than a van der Waals bond (<5 kJ/mol), and they are about the energy of hydrogen bonds (10–40 kJ/mol) [26]. The strong aurophilic interaction is ascribed to the relativistic effect of gold. In chemistry, relativistic effect means when the electrons with high speed move close to a heavy nucleus, the mass increases consequently, and so does the effective nuclear charge [27]. Thus the less diffuse orbitals (s and p) contract radially and the orbital energy is stabilized, leading to a stronger shielding of the nuclear attraction. The more diffuse orbitals (d and f) expand radially and results in a destabilization of the orbital energy. Gold has a larger relativistic effect than any other element with $Z < 100$ [28]. The tendency of Au(I) to form larger clusters via a weak interaction is due to the stabilization of molecular orbitals derived from the filled 5d atomic orbitals by configuration mixing with empty molecular orbitals from 6s or 6p atomic orbitals [29].

Inspired by the Au(I) compounds, our group has reported the first example of ligand-unsupported Ag(I) complex with argentophilic interaction, $\text{TI}[\text{Ag}(\text{CN})_2]$ [30]. X-ray crystallography, luminescence, and temperature-dependent Raman spectra measurements were carried out. The crystal structure results show that the Ag–Ag bond distance is 3.11 Å and the low energy Ag–Ag vibrational frequency of about 75–125 cm^{-1} given by Raman indicates the presence of direct argentophilic interaction in $\text{TI}[\text{Ag}(\text{CN})_2]$. Since then, our group has reported a series of d^{10} metal cyano compounds in nano systems [31–41]. We found that due to the formation of different size exciplexes, these nano systems show interesting photophysical and photochemical behaviors, such as emission tunability, thermochromism, and optical memory. Luminescence of these systems not surprisingly depends upon the content of cyanometallic compounds, similar to excimers in aqueous solution. In this paper, we

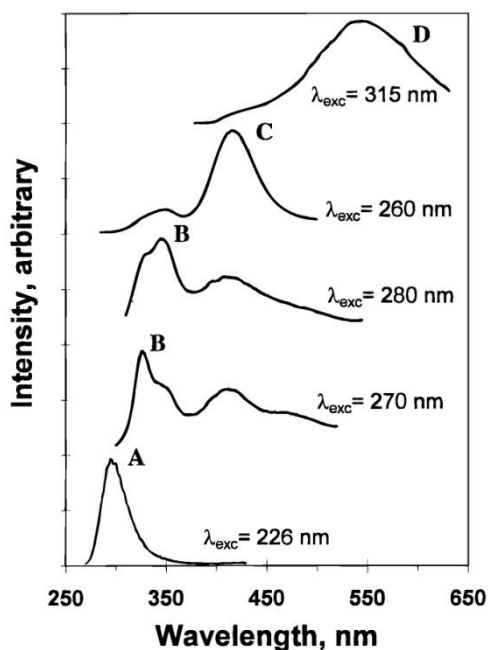
review the research work concerning $\text{Ag}(\text{CN})_2^-$, $\text{Au}(\text{CN})_2^-$, and $\text{Cu}(\text{CN})_2^-$ nano systems, which possess interesting luminescence properties.

2. $\text{Ag}(\text{CN})_2^-$ Excimers and Exciplexes

The photoluminescence of solid state $\text{Tl}[\text{Ag}(\text{CN})_2]$ indicates the existence of argentophilicity in $\text{Ag}(\text{I})$ compounds [30]. The $\text{Ag}-\text{Ag}$ interaction is believed to result in the formation of $^*[\text{Ag}(\text{CN})_2^-]$ excimers in the bulky state. We carried out a study focusing on the $^*[\text{Ag}(\text{CN})_2^-]_n$ in the nano state by doping $\text{Ag}(\text{CN})_2^-$ in KCl hosts [31–34,39]. The $\text{KAg}(\text{CN})_2/\text{KCl}$ nano systems were prepared by a simple slow evaporation method and the concentration was determined using atomic absorption method.

Figure 1 shows the emission peaks for the $\text{KAg}(\text{CN})_2/\text{KCl}$ single crystal. Multiple emission peaks at 295, 327, 345, 417, and 548 nm were observed for corresponding excitation wavelengths. These luminescence peaks are labeled as A, B, C, and D respectively, as indicated in Figure 1. For each emission band, the corrected excitation spectra were compared to the absorption of a $\text{KAg}(\text{CN})_2$ aqueous solution. The $\text{KAg}(\text{CN})_2$ solution absorbs at 196 nm, ascribed to a metal-to-ligand charge transfer process. However, the excitation maxima for A–D bands are at much lower energy and the homometallic interaction is believed to play an important role in the large red-shift of the excitation peaks.

Figure 1. Exciplex tuning by site-selective excitation: emission spectra of a $\text{KAg}(\text{CN})_2/\text{KCl}$ crystal at 77 K with different excitation wavelengths. Intensities are not comparable between different spectra. (Reprinted with permission from [31]. Copyright 1998 American Chemical Society.)



To better understand the argentophilic interaction, electronic structure calculations using both extend Hückel and *ab initio* methods were conducted for a monomer, dimer and trimer doped in KCl hosts. As shown in Figure 2, a $\text{Ag}(\text{CN})_2^-$ monomer is present in the KCl cubic unit cell with substituting Ag^+ and CN^- for K^+ and Cl^- , thus the total charge of this system is unchanged. For dimers,

there are three different configurations, eclipsed, perpendicular, and offset-eclipsed, which all have linear $\text{Ag}(\text{CN})_2^-$ units. Calculations for four trimers with linear and angular arrangements respectively were carried out as well.

Figure 2. Structure of a unit cell of KCl with a defect created by doping two adjacent $\text{Ag}(\text{CN})_2^-$ ions. In the defect, the Ag^+ and CN^- ions are shown to occupy the K^+ and Cl^- sites, respectively. (Reprinted with permission from [31]. Copyright 1998 American Chemical Society.)

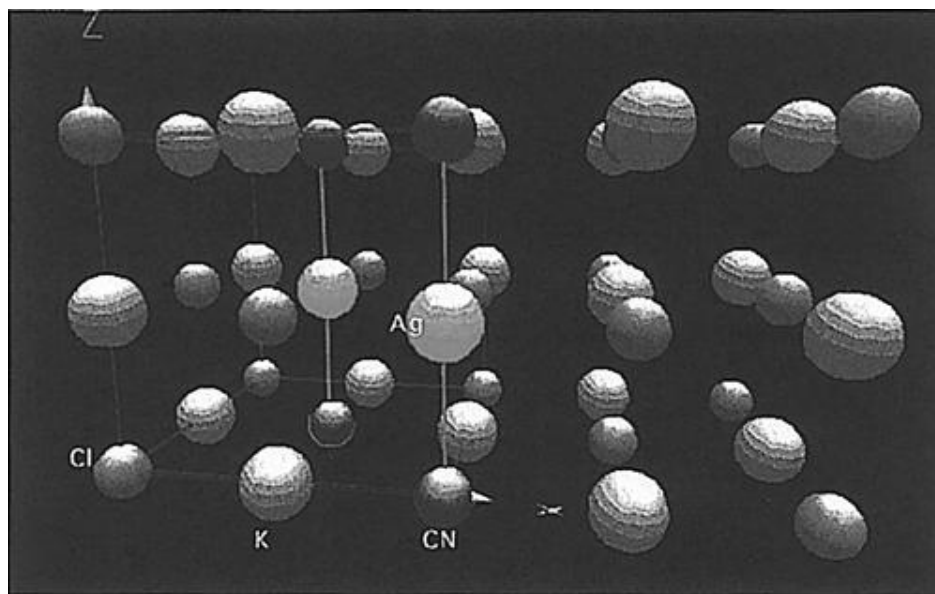


Table 1 summarizes the calculated results for the equilibrium distance, binding energy, HOMO-LUMO gap and overlap population for $[\text{Ag}(\text{CN})_2^-]_n$ nanoclusters in ground and excited states. The bond distance between two Ag atoms is shorter in the excited state than in the ground state. In addition, the binding energy and the overlap population also increase significantly in the excited states in comparison with the ground states. These are consistent with the behavior of excimer and exciplex. The interaction between monomer units is stronger in the excited state, which results in a stable excited dimer, e.g., excimer. The multiple HOMO-LUMO gap energies by calculation are in agreement with the different luminescence bands (A to D) observed experimentally. Interestingly, the HOMO-LUMO gap show a trend that with an increase in the number of interacting $\text{Ag}(\text{CN})_2^-$, the emission energy decreases. This explains the exciplex tuning behavior and the different bands A, B, C, and D are tentatively assigned to excimer, *cis*-localized exciplexes, *trans*-localized exciplexes, and delocalized exciplexes respectively. The *ab initio* calculation results for all $[\text{Ag}(\text{CN})_2^-]_n$ nanoclusters indicate an antibonding HOMO to bonding LUMO transition, which is also favorable for the formation of excimers and exciplexes.

Table 1. Summary of the Results of Extended Hückel Calculations for the Ground and Excited States of Oligomeric Species of Dicyanoargentate(I). (Adapted with permission from [31]. Copyright 1998 American Chemical Society.)

Species	[S]	[S] ₂ (<i>ec</i>)	*[S] ₂ (<i>ec</i>)	[S] ₂ (<i>st</i>)	*[S] ₂ (<i>TI,st</i>)	[S] ₃ (<i>TI,ec</i>)	*[S] ₃ (<i>TI,ec</i>)	[S] ₃ (<i>TI,st</i>)	*[S] ₃ (<i>TI,st</i>)	[S] ₃ (<i>TI,ec</i>)	*[S] ₃ (<i>TI,ec</i>)
Ag–Ag eq. diet, A	8.00 ^d	3.58	3.00	2.88	2.39	3.49	3.09	2.79	2.46	3.54	3.15
Binding energy, eV	0.00	0.13	1.12	0.22	1.32	0.33	1.47	0.61	2.00	0.29	1.14
H–L gap, eV	4.95	4.37	3.98	4.28	4.13	4.00	3.55	3.73	3.46	4.17	3.83
O.P. (Ag–Ag)	0.000	0.003	0.034	0.069	0.089	−0.008	0.027	0.039	0.079	0.003	0.048

The Ag(CN)₂[−]/KCl nano system has an extreme wide luminescence tuning range over 18,000 cm^{−1}, compared to some other systems [42–44]. This new optical behavior is referred to as exciplex tuning, in which the exciplex means excited state oligomers, not limited to dimers. The photoluminescence of the crystal can also be tuned by the content of the Ag in the host [32]. The higher energy bands are predominant for lower silver concentration whereas the spectra for higher silver concentration are mostly of lower energy bands. This further confirms the existence of different size nanoclusters in the doped system and the time-resolved luminescence spectra suggest energy transfer processes from dimers to trimers. The increase of trimer luminescence intensity is related to higher statistical population of trimers in Ag concentrated crystals and more acceptors for the energy transfer.

In addition to the novel exciplex tuning behavior, the Ag(CN)₂[−]/KCl nano system exhibits interesting thermochromism phenomena [33]. Figure 3 shows the emission spectra of a KCl/KAg(CN)₂ crystal at different temperatures. At room temperature, only one band (A) is observed while excited at 235 nm. However, as the temperature is cooled down to liquid nitrogen temperature (~77 K), band A almost disappears and a strong emission band C at lower energy appears. As the temperature is further decreased to 12 K, the emission spectra show predominantly band B at intermediate energy. Since the luminescence pattern changes dramatically with temperature, the possible cause relating to the Ag–Ag bond distance change is excluded. Another possibility that these emission bands are dependent on fluorescence and phosphorescence is also ruled out, because all the emission bands have a lifetime of microsecond magnitude. Therefore, the thermochromism behavior is due to some major structural changes. A kinetic model based on “normal” and back energy transfer is proposed. At liquid helium temperature, no energy transfer is involved and the luminescence is only from direct excitation. With temperature increasing to 80 K, “normal” energy transfer processes from high energy nanoclusters to low energy ones prevail and thus band C intensity increases in this temperature range. However, a further temperature increase leads to back energy transfer with reverse direction between nanoclusters. The back energy transfer is from low energy to high energy, which is not thermodynamically favorable. The higher activation energy than that of normal energy transfer is compensated by higher temperature, e.g., the back energy is significant at higher temperatures. In addition to KCl, different alkali halides, such as NaCl, NaBr, KBr, and NaF were used to study the host effect. Similar experimental results were obtained except for NaF, which is likely due to the small lattice size leaving no space for the Ag(CN)[−] clusters.

Figure 3. Emission spectra of a KCl/KAg(CN)₂ crystal as a function of temperature and excitation wavelength. Thin and thick curves represent spectra obtained with excitation wavelengths of 235 and 270 nm, respectively. Intensities are comparable between spectra at the same temperature but not comparable between spectra at different temperatures. (Reprinted with permission from [33]. Copyright 2000 American Chemical Society).

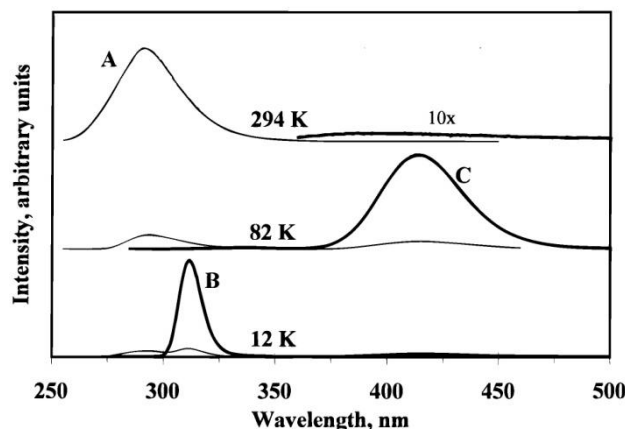
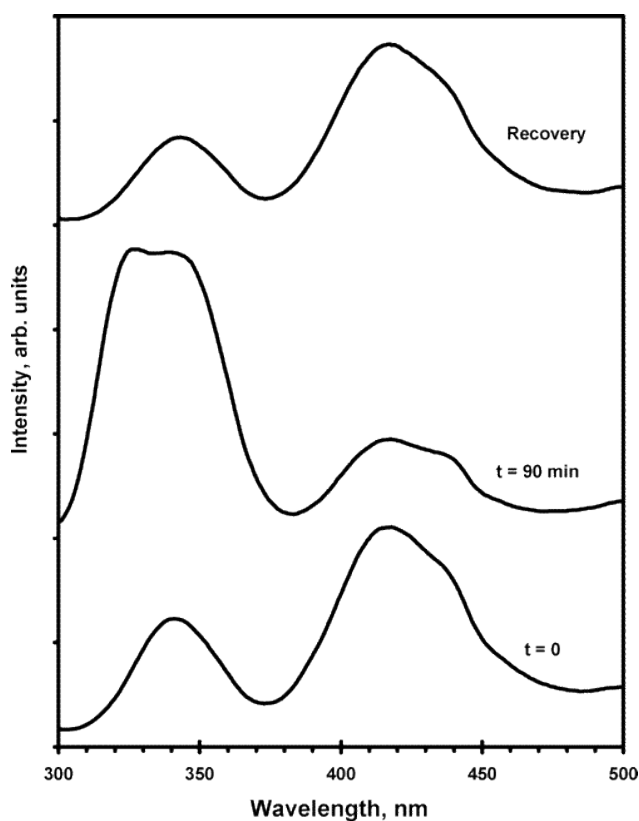


Figure 4. Emission spectra *versus* 266 nm laser irradiation time at 77 K for batch 1 of [Ag(CN)₂]⁻/KCl crystals. All spectra were scanned with 275 nm excitation. Note the dominance of the short-wavelength bands following irradiation at 77 K and the regeneration of the original spectrum in the recovery step. (Reprinted with permission from [39]. Copyright 2000 American Chemical Society.)



Optical memory is another interesting property resulting from the presence of the nanoclusters in the doped KCl host [39]. As shown in Figure 4, the $\text{Ag}(\text{CN})_2^-/\text{KCl}$ crystal show two emission peaks at 77 K. After irradiation at 266 nm for 90 min, the emission spectra have a significant change with the intensity of high energy peak increasing whereas the low energy peak intensity decreasing. Then, when the crystal is brought up to a warm temperature and cooled down again to 77 K again, the emission pattern recovers back to where it was at the beginning. In the whole process, acquiring emission spectra is “read”, irradiating laser beam on the crystal is “write”, and changing the temperature leads to “erase”. Therefore, this is a reversible write/read/erase optical memory behavior, which is similar to the research done by Zink and coworkers [45–47]. During the laser irradiations, the nanoclusters are excited and the distribution of different size excimers and exciplexes is changed, leading to the luminescence intensity change in the emission spectra. The kinetic study was conducted for every five min of laser irradiation and the activation energy was extrapolated via the emission peak intensity *versus* the logarithm of time. The obtained activation energy around 261 J/mol suggests a fast energy transfer between these $[\text{Ag}(\text{CN})_2^-]_n$ excimers and exciplexes.

3. $\text{Au}(\text{CN})_2^-$ Excimer and Exciplexes

Our group has carried out a study on $\text{Ag}(\text{CN})_2^-$ and $\text{Au}(\text{CN})_2^-$ in aqueous as well as other organic solutions and observed non-Beer’s law behavior of the absorption for different concentrations of solution, as shown in Figure 5 [35,36]. The luminescence spectra of $\text{K}[\text{Au}(\text{CN})_2]$ aqueous solution at room temperature and 77 K exhibit different emission peaks and the pattern depends upon the excitation wavelength. Theoretical calculations indicate the energy gap between the HOMO and LUMO decreases as the oligomer size increases. Both experimental and theoretical results suggest the presence of $[\text{Au}(\text{CN})_2^-]_n$ excimers and exciplexes. Consequently, investigations on $\text{KAu}(\text{CN})_2$ doped in an alkali halide host was conducted to further understand the close-shell interaction between $\text{Au}(\text{I})$ complexes [38].

Figure 5. Absorption spectra *versus* concentration of $\text{K}[\text{Au}(\text{CN})_2]$ in aqueous solutions at ambient temperature. (Reprinted with permission from [35]. Copyright 2002 American Chemical Society.)

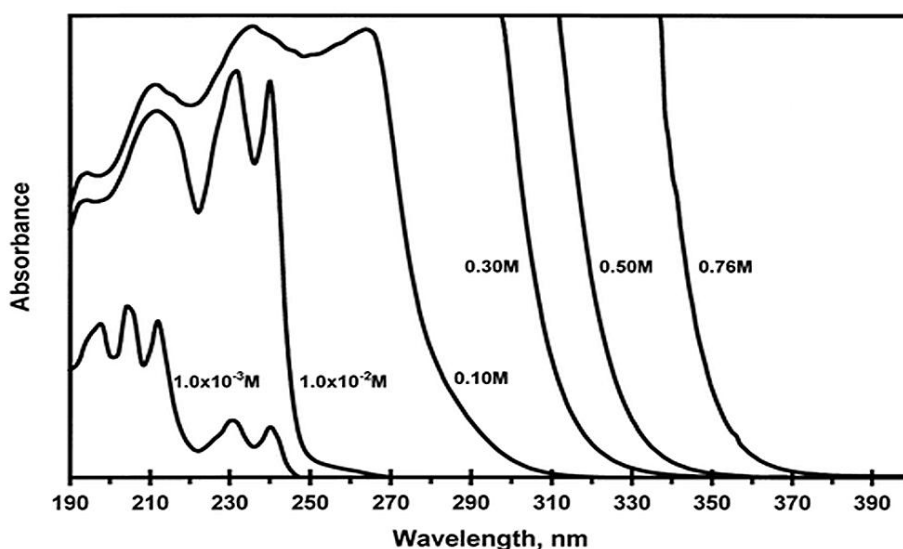


Figure 6 shows the emission spectra of a $\text{KAu}(\text{CN})_2/\text{KCl}$ single crystal at 77 K. Same as the argentocyanide/alkali halide system, the $\text{Au}(\text{CN})_2^-/\text{KCl}$ also exhibit exciplex tuning behavior. The excitation ranges from 270 nm to 350 nm and the emission peaks are at 335, 390, and 425 nm respectively. However, the pure $\text{KAu}(\text{CN})_2$ crystal only shows one emission peak at 390 nm with different excitation wavelengths. Table 2 lists the emission maxima for $\text{KAu}(\text{CN})_2$ in an alkali halide host and aqueous solution, as well as the corresponding assignments. The high energy emission peak at 275–285 nm in $\text{KAu}(\text{CN})_2$ aqueous solution was not observed for the solid state, implying no $\text{Au}(\text{CN})_2^-$ monomer species is present in the doped KCl crystal. However, for the aqueous solution, due to the limit of concentration, low energy emission peak from the larger size of $[\text{Au}(\text{CN})_2^-]_n$ does not exist. These results are in agreement with a model where the homometallic interactions between different $\text{Au}(\text{CN})_2^-$ units form excimers and exciplexes. The lifetime measurements show microsecond magnitude phosphorescence, suggesting a metal to ligand charge-transfer process. In addition, Raman spectroscopy results provide further evidence for the formation of different nanoclusters in the doped crystal. A pure $\text{KAu}(\text{CN})_2$ crystal exhibits only one peak in the cyanide stretching region (about 2176 cm^{-1}), whereas the doped crystals have additional peaks at 2169 and 2189 cm^{-1} . This is consistent with the photoluminescence results. The homometallic interaction in $[\text{Au}(\text{CN})_2^-]_n$ nanoclusters affects the back bonding from gold to the cyanide ligand, which results in the shift of cyanide stretching frequency.

Figure 6. Emission spectra of a single crystal of $\text{KAu}(\text{CN})_2/\text{KCl}$ at 77 K with different excitation wavelengths. (Reprinted with permission from [38]. Copyright 2002 American Chemical Society.)

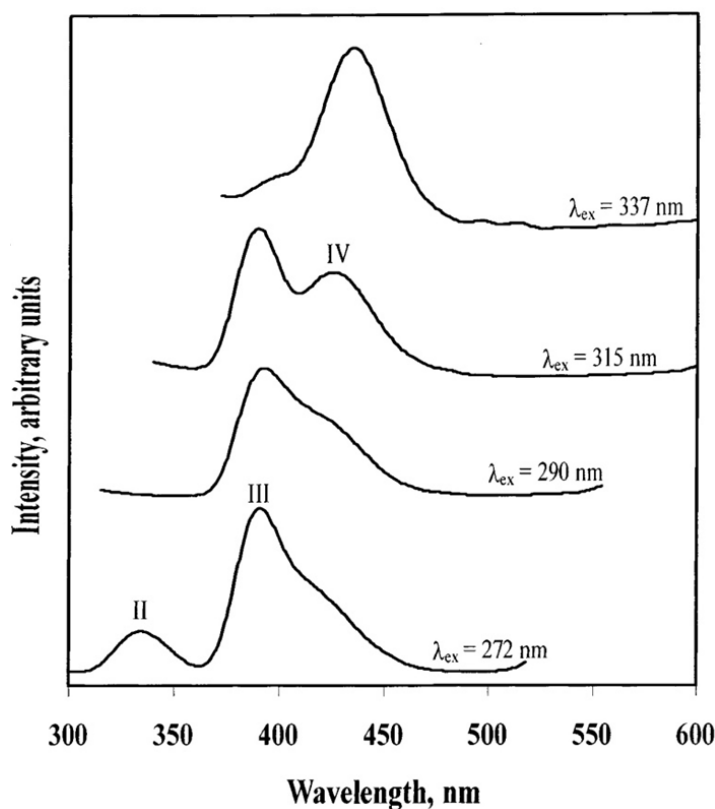


Table 2. General Qualitative Assignment of the Emission Bands Observed in Solids and Solutions of Au(CN)₂-Species. (Adapted with permission from [38]. Copyright 2002 American Chemical Society.)

band	solids, $\lambda_{\max}^{\text{em}}, \text{nm}$	solutions $\lambda_{\max}^{\text{em}}, \text{nm}$	assignment
I	–	275–285	*[Au(CN) ₂] [–] ₂
II	320–355	320–350	bent *[Au(CN) ₂] [–] ₃
III	370–395	380–390	linear *[Au(CN) ₂] [–] ₃
IV	420–450	420–440	*[Au(CN) ₂] [–] ₄
V	–	455–490	*[Au(CN) ₂] [–] _n ^a
VI	600–640	–	*[Au(CN) ₂] [–] _n

^a *[Au(CN)₂][–]_n represents delocalized exciplexes.

Theoretical calculations were conducted using Extended Hückel methods for [Au(CN)₂][–] monomer, dimer, trimer, and tetramer. The energy results of the ground state and the first excited-state results for these oligomers show that with the increase of the size, the binding energy between [Au(CN)₂][–] units increase and the HOMO-LUMO gap decreases. All the results indicate the bonding between Au-Au is stronger in the excited state and this confirms the existence of [Au(CN)₂][–]_n excimers and exciplexes. For the trimer, the geometry also plays an important role and leads to different emission centers. The dynamics of [Au(CN)₂][–]_n oligomer geometry changes have been studied by ultrafast spectroscopic experiments [48]. The time-resolved results show direct evidence of a shortening of Au-Au distance and further support the formation of [Au(CN)₂][–]_n nanoclusters.

4. Cu(CN)₂[–] Excimer and Exciplexes

As the last member in the coinage group, copper has a smaller relativistic effect than gold and silver and the homometallic interaction between Cu(I) compounds should be less [28]. Moreover, most of the reported luminescent Cu(I) complexes are cationic with chelating imine ligands or bisphosphine ligands or cuprous clusters [49]. However, our group has reported photophysical and photochemical properties of anionic Cu(CN)₂[–] doped in alkali halide hosts which resulted from the close-shell interaction of Cu(I) [41].

Unlike pure KAg(CN)₂ and KAu(CN)₂ which have linear M(CN)₂[–], the dicyanocuprate salts have a local trigonal Cu(CN)₂[–] structure. X-ray diffraction (XRD) results indicate that both NaCu(CN)₂ · 2H₂O and KCu(CN)₂ have a polymeric-chain structure. NaCu(CN)₂ has zigzag CuCN chains linked to [Na(H₂O)₂]⁺ polyhedra and the copper has a trigonal-planar structure, with two bridge cyanides for the polymeric chain and one for the [Na(H₂O)₂]⁺ polyhedra. However, in KCu(CN)₂, the polymeric chain is along a two-fold screw axis and the three-coordination of copper is not planar. However, when NaCu(CN)₂ and KCu(CN)₂ is doped in alkali halide hosts, the copper(I) cation becomes six-coordinated within the crystal field. With two cyanides and four surrounding halide atoms; the [Cu(CN)₂X₄]^{5–} (X for halides) has a local D_{4h} symmetry. Figure 7 gives IR and Raman spectra in the CN stretching region for the pure and NaCl doped dicyanocuprate(I) crystals. The pure NaCu(CN)₂ · 2H₂O, KCu(CN)₂ have two CN vibrational modes in both IR and Raman, which is due to the local C_{2v} symmetry of trigonal Cu(CN)₂[–]. For the doped crystals, the same results were observed for both dicyanocuprate

salts, suggesting the linear structure in NaCl hosts. Same results were obtained for NaBr and KBr doped $\text{Cu}(\text{CN})_2^-$ crystals. This structural change is also confirmed by UV-vis diffuse reflectance and aqueous solution absorption spectroscopy experiments.

Figure 7. The ν_{CN} region IR and Raman spectra of pure $\text{NaCu}(\text{CN})_2 \cdot 2\text{H}_2\text{O}$, $\text{KCu}(\text{CN})_2$ and doped in NaCl. (Reprinted with permission from [41]. Copyright 2012 American Chemical Society.)

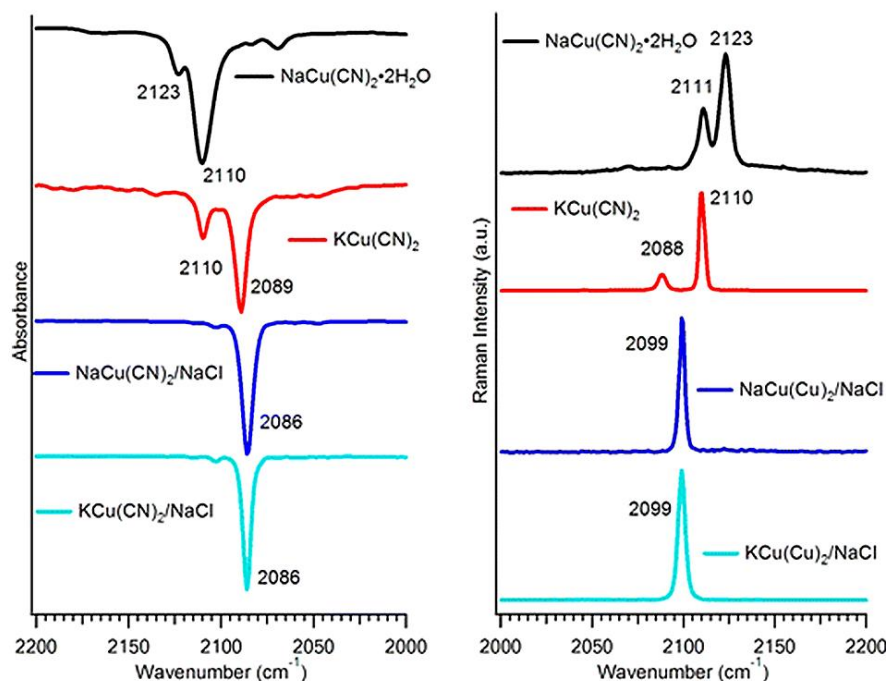
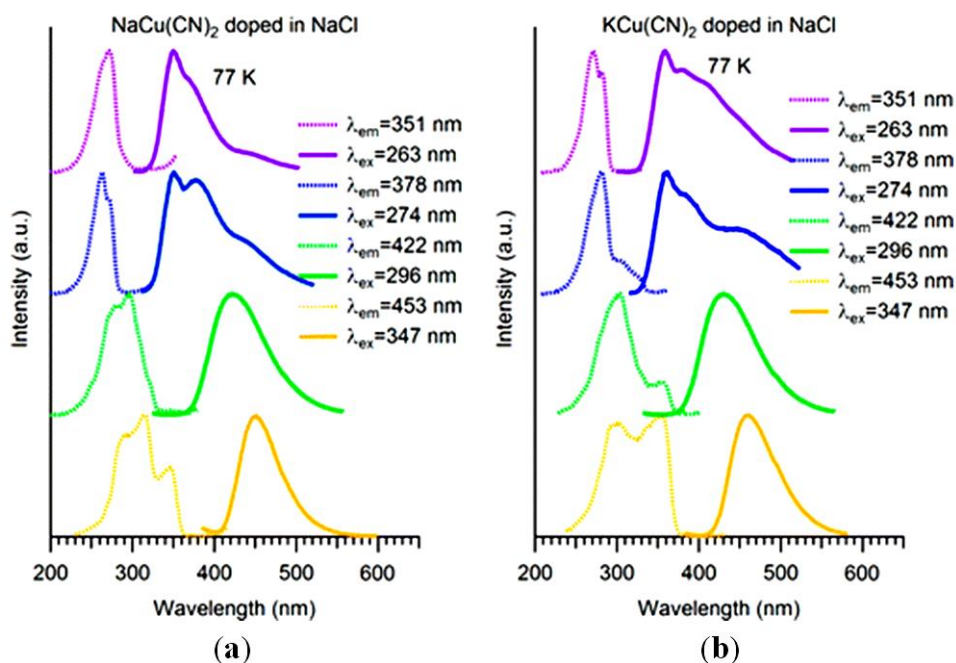


Figure 8. Luminescence spectra at 77 K of (a) $\text{NaCu}(\text{CN})_2$ and (b) $\text{KCu}(\text{CN})_2$ doped in NaCl. (Reprinted with permission from [41]. Copyright 2012 American Chemical Society.)

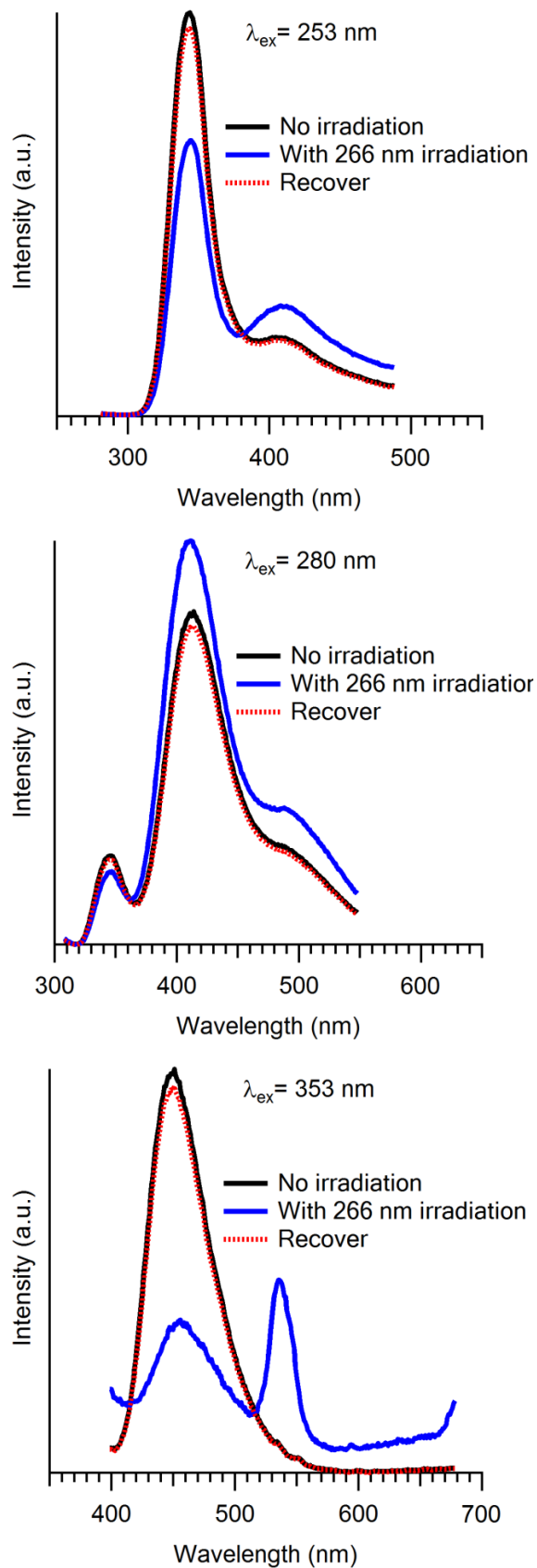


The $\text{Cu}(\text{CN})_2^-$ doped in alkali halide host systems show a series of interesting photophysical and photochemical properties. Similar to $\text{Au}(\text{CN})_2^-$ and $\text{Ag}(\text{CN})_2^-$, the dicyanocuprate ion in sodium chloride crystal exhibits exciplex tuning, as indicated in Figure 8. Both $\text{NaCu}(\text{CN})_2 \cdot 2\text{H}_2\text{O}$ and $\text{KCu}(\text{CN})_2$ in NaCl show the same luminescence pattern, which provides further evidence for the linear structure of $\text{Cu}(\text{CN})_2^-$ in doped hosts. Other alkali halides, such as NaBr and KBr , were also used and the result was that all the crystals have exciplex tuning. For each host, both $\text{NaCu}(\text{CN})_2 \cdot 2\text{H}_2\text{O}$ and $\text{KCu}(\text{CN})_2$ give the same luminescence pattern. The intensity of emission peaks depends upon the concentration of the copper in these crystals. The relative peak intensity of low energy peak to high energy peak increases with higher $\text{Cu}(\text{CN})_2^-$ content. As we have discussed for $\text{Ag}(\text{CN})_2^-/\text{KCl}$ crystals, the lower energy peaks are assigned to larger size nanoclusters, therefore in the copper case, the increase of $\text{Cu}(\text{CN})_2^-$ concentration consequently leads to the formation of more large size oligomers and the lower energy peaks arise.

Thermochromism and optical memory were also observed for $\text{Cu}(\text{CN})_2^-$ doped crystals. Between 77 and 200 K, all the peak intensity decreases due to the quenching with increasing temperature. However, above 200 K, the intensity of higher energy peaks abruptly increases and the lower energy peak almost disappears. This is ascribed to the population change during the temperature increasing; the large size nanoclusters break into small size monomers and dimers, which take place between 200 and 250 K. After the reaction is completed, the distribution of nanoclusters no longer changes and the peak intensity is only affected by the temperature. The optical memory experiment was conducted in three steps: (1) the doped crystal is cooled down to liquid nitrogen temperature and during the cooling process, the crystal is irradiated by the 266 nm laser, which is the writing; (2) the emission spectra are recorded at 77 K, the reading; and (3) the crystal is heated up to the room temperature and then cooled down to 77 K again. The luminescence spectra are shown in Figure 9. Excimer and exciplex are more stable and the metal-metal distance is shorter for excited states. The laser irradiation promotes $\text{Cu}(\text{CN})_2^-$ ions into an excited state and thus form larger size nanoclusters. With the temperature decrease, they are frozen in their positions, which leads to the distribution change of different nanoclusters.

Theoretical density functional calculations were carried out for monomers and possible dimers and the possible configurations are shown in Scheme 1. The calculated electron density results give a major metal-to-ligand charge transfer (MLCT) mixed with ligand-to-ligand charge transfer (LLCT) transition and this is in agreement with the long life time (μs) of all emission peaks, suggesting the phosphorescence process. Figure 10 gives the isodensity map of some of the $[\text{Cu}(\text{CN})_2^-]_n$ in alkali halide hosts. The optimized structure for monomers and dimers were obtained in the ground state and the first excited triplet state. Comparing the bond distances between the ground state and the first excited triplet state, we find that the $\text{Cu}-\text{C}$ bond distances contract and the $\text{C}\equiv\text{N}$ bond distances expand, which is in accordance with the MLCT transition. Time-dependent DFT calculation results show the absorption and emission energies follow the trend that with the size of nanoclusters increase, the corresponding energies red shift. This is also observed from the experimental results. Atomistic calculations show that the potassium salts have greater bridging state selectivity and more favorable oligomerization energy than that of sodium salts. Bromide salts show a slightly greater bridging state selectivity than chloride salts.

Figure 9. Emission spectra of $\text{Cu}(\text{CN})_2^-$ doped in KBr at 77 K without laser irradiation (black solid), with 266 nm laser irradiation (blue solid), and recover, e.g., heat to room temperature then cool down to 77 K without laser irradiation (red dashed). (Reprinted with permission from [41]. Copyright 2012 American Chemical Society.)



Scheme 1. Dimeric configurations of $\text{Cu}_2(\text{CN})_4\text{X}_6$ or $7]^{8-}$ or $9-$ ions. (Reprinted with permission from [41]. Copyright 2012 American Chemical Society.)

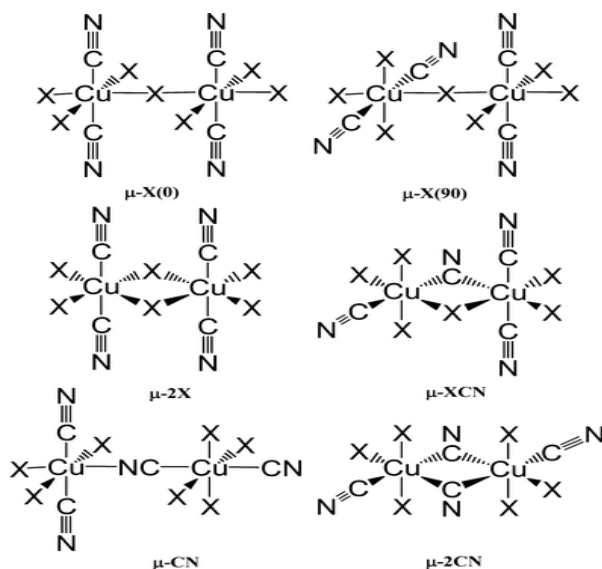
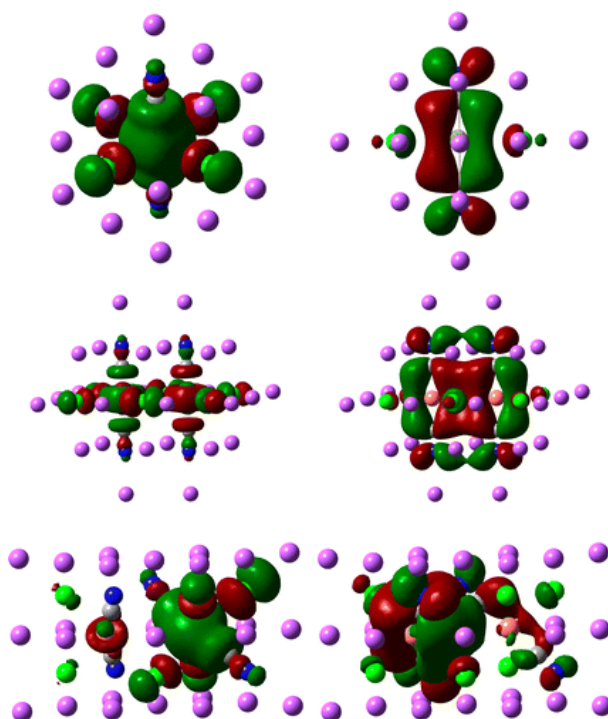


Figure 10. Isodensity of HOMO (left) and LUMO (right) for $\text{Cu}(\text{CN})_2^-$ monomers (top), $\mu\text{-Cl}_2$ dimers (middle) and $\mu\text{-ClCN}$ dimers (bottom). (Reprinted with permission from [41]. Copyright 2012 American Chemical Society.)



5. Conclusions

The dicyano compounds of coinage metals, Ag, Au, and Cu doped in alkali halide hosts show examples of close-shell homometallic interactions, which results in a series of interesting photophysical and photochemical properties. These nanoclusters are typical excimers and exciplexes, e.g., more stable at the excited states. Especially for copper, the $\text{Cu}(\text{CN})_2^-$ in alkali halide crystals are

unique examples for luminescent anionic Cu(I) compounds. The population of different nanoclusters changes with the concentration, temperature, and laser irradiation. Lifetime results of microsecond magnitude suggest phosphorescence and are consistent with the calculation results, which gives a MLCT transition with slightly LLCT process. The exciplex tuning gives a range as wide as $18,000\text{ cm}^{-1}$ and the strong phosphorescence has possible application for solid state lasers. Thermochromism and optical memory properties can be used to make new photosensors and memory devices.

Acknowledgments

This work was supported by the National Science Foundation (CHE-0443345).

Conflicts of Interest

The authors declare no conflict of interest.

References

1. Stevens, B.; Hutton, E. Radiative life-time of the pyrene dimer and the possible role of excited dimers in energy transfer processes. *Nature* **1960**, *186*, 1045–1046.
2. Rayleigh, L. Series of emission and absorption bands in the mercury spectrum. *Proc. R. Soc. A* **1927**, *116*, 702–719.
3. Hopefield, J.J. Certain effects accompanying electron diffraction. *Phys. Rev.* **1930**, *35*, 1133–1134.
4. Birks, J.B. Excimers. *Rep. Prog. Phys.* **1975**, *38*, 903–974.
5. Förster, T.H.; Kasper, K. Ein Konzentrationsumschlag der Fluoreszenz. *Z. Phys. Chem. (N.F.)* **1954**, *1*, 275–277.
6. Förster, T.H.; Kasper, K. Ein Konzentrationsumschlag der Fluoreszenz des Pyrens. *Z. Elektrochem.* **1955**, *59*, 976–980.
7. Ivanova, T.V.; Mokeeva, G.A.; Sveshnikov, B.Y.A. Dependence of the fluorescence of benzene, toluene, and p-xylene solutions on the concentration of fluorescent substance. *Opt. Spectrosc.* **1962**, *12*, 325–328.
8. Döller, E.; Förster, T.H. Der Konzentrationsumschlag der Fluoreszenz des Naphthalins. *Z. Phys. Chem. (N.F.)* **1962**, *31*, 274–277.
9. Birks, J.B.; Christophorou, L.G. Excimer fluorescence of aromatic hydrocarbons in solution. *Nature* **1962**, *194*, 442–444.
10. Birks, J.B.; Christophorou, L.G. Resonance interactions of fluorescent organic molecules in solution. *Nature* **1962**, *196*, 33–35.
11. Birks, J.B.; Christophorou, L.G. “Excimer” fluorescence. IV. Solution spectra of polycyclic hydrocarbons. *Proc. R. Soc. A* **1964**, *277*, 571–582.
12. Miller, J.C.; Andrews, L. Absorption and laser-excited fluorescence spectra of matrix-isolated metal van der waals dimmers. *Appl. Spectrosc. Rev.* **1980**, *16*, 1–42.
13. Kunkely, H.; Vogler, A. Photoluminescence of $[\text{Pt}^{\text{II}}(4,7\text{-diphenyl-1,10-phenanthroline})(\text{CN})_2]$ in solution. *J. Am. Chem. Soc.* **1990**, *112*, 5625–5627.

14. Nagle, J.K.; Brennan, B.A. Luminescent exciplex formation involving Tetrakis(μ -diphosphito) diplatinate(II) and -Thallium(I) in aqueous solution. *J. Am. Chem. Soc.* **1988**, *110*, 5931–5932.
15. Pettijohn, C.N.; Jochnowitz, E.B.; Chuong, B.; Nagle, J.K.; Vogler, A. Luminescent Excimers and exciplexes of Pt^{II} compounds. *Coord. Chem. Rev.* **1998**, *171*, 85–92.
16. Harvey, P.D.; Gray, H.B. Low-lying singlet and triplet electronic excited states of binuclear (d^{10} - d^{10}) Palladium(0) and Platinum(0) complexes. *J. Am. Chem. Soc.* **1988**, *110*, 2145–2147.
17. Che, C.-M.; Kwong, H.-L.; Yam, V.W.-W.; Cho, K.C. Spectroscopic properties and redox chemistry of the phosphorescent excited state of $[\text{Au}_2(\text{dppm})_2]^{2+}$. *J. Chem. Soc. Chem. Commun.* **1989**, 885–886.
18. King, C.; Wang, J.-C.; Khan, M.N.I.; Fackler, J.P., Jr. Luminescence and metal-metal interactions in binuclear Gold(I) compounds. *Inorg. Chem.* **1989**, *28*, 2145–2149.
19. Perreault, D.; Drouin, M.; Michel, A.; Miskowski, V.M.; Schaefer, W.P.; Harvey, P.D. Silver and gold dimers. Crystal and molecular structure of $\text{Ag}_2(\text{dmpm})_2\text{Br}_2$ and $[\text{Au}_2(\text{dmpm})_2](\text{PF}_6)_2$ and relation between metal-metal force constants and metal-metal separations. *Inorg. Chem.* **1992**, *31*, 695–702.
20. Fu, W.-F.; Chan, K.-C.; Miskowski, V.M.; Che, C.-M. The intrinsic $^3[\text{d}\sigma^*\text{p}\sigma]$ emission of binuclear Gold(I) complexes with two bridging diphosphane ligands lies in the near UV; Emissions in the visible region are due to exciplexes. *Angew. Chem. Int. Ed.* **1999**, *38*, 2783–2785.
21. Leung, K.-H.; Phillips, D.L.; Tse, M.-C.; Che, C.-M.; Miskowski, V.M. Resonance raman investigation of the Au(I)-Au(I) interaction of the $^1[\text{d}\sigma^*\text{p}\sigma]$ excited state of $\text{Au}_2(\text{dcpm})_2(\text{ClO}_4)_2$. *J. Am. Chem. Soc.* **1999**, *121*, 4799–4803.
22. Che, C.-M.; Mao, Z.; Miskowski, V.M.; Tse, M.-C.; Chan, C.-K.; Cheung, K.-K.; Phillips, D.L.; Leung, K.-H. Cuprophilicity: Spectroscopic and structural evidence for Cu–Cu bonding interactions in luminescent dinuclear Copper(I) complexes with bridging diphosphane ligands. *Angew. Chem. Int. Ed.* **2000**, *39*, 4084–4088.
23. Che, C.-M.; Tse, M.-C.; Chan, M.C.W.; Cheung, K.-K.; Phillips, D.L.; Leung, K.-H. Spectroscopic evidence for argentophilicity in structurally characterized luminescent binuclear Silver(I) complexes. *J. Am. Chem. Soc.* **2000**, *122*, 2464–2468.
24. Fu, W.-F.; Chan, K.-C.; Cheung, K.-K.; Che, C.-M. Substrate-binding reactions of the $^3[\text{d}\sigma^*\text{p}\sigma]$ Excited state of binuclear Gold(I) complexes with bridging bis(dicyclohexylphosphino)methane ligands: Emission and time-resolved absorption spectroscopic studies. *Chem. Eur. J.* **2001**, *7*, 4656–4664.
25. Zhang, H.-X.; Che, C.-M. Auophilic attraction and luminescence of binuclear Gold(I) complexes with bridging phosphine ligands: *Ab initio* study. *Chem. Eur. J.* **2001**, *7*, 4887–4893.
26. Pyykkö, P. Strong closed-shell interactions in inorganic chemistry. *Chem. Rev.* **1997**, *97*, 597–636.
27. Rose, J.; Grant, I.P.; Pyper, N.C. The direct and indirect effects in the relativistic modification of atomic valence orbitals. *J. Phys. B* **1978**, *11*, 1171–1176.
28. Pyykkö, P. Relativität, gold, wechselwirkungen zwischen gefüllten schalen und CsAu-NH_3 . *Angew. Chem.* **2002**, *114*, 3723–3728.
29. Vogler, A.; Kunkely, H. Absorption and emission spectra of tetrameric Gold(I) complexes. *Chem. Phys. Lett.* **1988**, *150*, 135–137.

30. Omary, M.A.; Webb, T.R.; Assefa, Z.; Shankle, G.E.; Patterson, H.H. Crystal structure, electronic structure, and temperature-dependent raman spectra of $\text{TI}[\text{Ag}(\text{CN})_2]$: Evidence for ligand-unsupported argentophilic interactions. *Inorg. Chem.* **1998**, *37*, 1380–1386.
31. Omary, M.A.; Patterson, H.H. Luminescent homoatomic exciplexes in Dicyanoargentate(I) ions doped in Alkali halide crystals. 1. “Exciplex tuning” by site-selective excitation. *J. Am. Chem. Soc.* **1998**, *120*, 7696–7705.
32. Omary, M.A.; Hall, D.D.; Shankle, G.E.; Siemiarczuk, A.; Patterson, H.H. Luminescent homoatomic exciplexes in Dicyanoargentate(I) ions doped in Alkali halide crystals. 2. “Exciplex tuning” by Varying the dopant concentration. *J. Phys. Chem. B* **1999**, *103*, 3845–3853.
33. Rawashdeh-Omary, M.A.; Omary, M.A.; Shankle, G.E.; Patterson, H.H. Luminescence thermochromism in Dicyanoargentate(I) ions doped in Alkali halide crystals. *J. Phys. Chem. B* **2000**, *104*, 6143–6151.
34. Patterson, H.H.; Kanan, S.M.; Omary, M.A. Luminescent homoatomic exciplexes in Dicyanoargentate(I) ions doped in Alkali halide crystals. “Exciplex tuning” by site-selective excitation and variation of the dopant concentration. *Coord. Chem. Rev.* **2000**, *208*, 227–241.
35. Rawashdeh-Omary, M.A.; Omary, M.A.; Patterson, H.H. Oligomerization of $\text{Au}(\text{CN})_2^-$ and $\text{Ag}(\text{CN})_2^-$ ions in solution via ground-state aurophilic and argentophilic bonding. *J. Am. Chem. Soc.* **2000**, *122*, 10371–10380.
36. Rawashdeh-Omary, M.A.; Omary, M.A.; Patterson, H.H.; Fackler, J.P., Jr. Excited-state interactions for $[\text{Au}(\text{CN})_2^-]_n$ and $[\text{Ag}(\text{CN})_2^-]_n$ Oligomers in solution. Formation of luminescent gold–gold bonded excimers and exciplexes. *J. Am. Chem. Soc.* **2001**, *123*, 11237–11247.
37. Kanan, S.M.; Kanan, M.C.; Patterson, H.H. Photophysical properties of Ag(I)-exchanged zeolite A and the photoassisted degradation of malathion. *J. Phys. Chem. B* **2001**, *105*, 7508–7516.
38. Hettiarachchi, S.R.; Rawashdeh-Omary, M.A.; Kanan, S.M.; Omary, M.A.; Patterson, H.H.; Tripp, C.P. Spectroscopic studies of “exciplex tuning” for Dicyanoaurate(I) ions doped in potassium chloride crystals. *J. Phys. Chem. B* **2002**, *106*, 10058–10064.
39. Hettiarachchi, S.R.; Patterson, H.H.; Omary, M.A. Write/read/erase with laser irradiation of Dicyanoargentate(I) doped and pure crystals. *J. Phys. Chem. B* **2003**, *107*, 14249–14254.
40. Baril-Robert, F.; Li, X.; Welch, D.A.; Schneider, B.Q.; O’Leary, M.; Larochelle, C.L.; Patterson, H.H. Site-selective excitation of “exciplex tuning” for luminescent nanoclusters of Dicyanoargentate(I) ions doped in different Alkali halide crystals. *J. Phys. Chem. C* **2010**, *114*, 17401–17408.
41. Li, X.; Pan, Z.; Welch, D.A.; Baril-Robert, F.; Pike, R.D.; Patterson, H.H. An unusual luminescent anionic Copper(I) system: Dicyanocuprate(I) ion in nano and bulky states. *J. Phys. Chem. C* **2012**, *116*, 26656–26667.
42. Cummings, S.D.; Eisenberg, R. Tuning the excited-state properties of Platinum(II) diimine dithiolate complexes. *J. Am. Chem. Soc.* **1996**, *118*, 1949–1960.
43. Yersin, H.; Gliemann, G. Spectroscopic studies of $\text{M}_x[\text{Pt}(\text{CN})_4] \cdot y\text{H}_2\text{O}$. *Ann. N.Y. Acad. Sci.* **1978**, *313*, 539–559.
44. Gliemann, G.; Yersin, H. Spectroscopic properties of the quasi one-dimensional Tetracyanoplatinate(II) compounds. *Struct. Bond.* **1985**, *62*, 87–153.

45. Hollingsworth, G.; Barrie, J.D.; Dunn, B.; Zink, J.I. Optical memory in Cu⁺-Doped β''-Alumina. *J. Am. Chem. Soc.* **1988**, *110*, 6569–6572.
46. Barrie, J.D.; Dunn, B.; Hollingsworth, G.; Zink, J.I. Optical spectroscopy of Copper(I) doped β''-Alumina. *J. Phys. Chem.* **1989**, *93*, 3958–3963.
47. Barrie, J.D.; Dunn, B.; Zink, J.I. Optical spectroscopy of Cu⁺/Ag⁺ Doped β''-Alumina. *J. Am. Chem. Soc.* **1990**, *112*, 5701–5706.
48. Iwamura, M.; Nozaki, K.; Takeuchi, S.; Tahara, T. Real-time observation of tight Au–Au bond formation and relevant coherent motion upon photoexcitation of [Au(CN)₂][−] oligomers. *J. Am. Chem. Soc.* **2013**, *135*, 538–541.
49. Armaroli, N.; Accorsi, G.; Cardinali, F.; Listorti, A. Photochemistry and photophysics of coordination compounds: Copper. *Top. Curr. Chem.* **2007**, *280*, 69–115.

© 2013 by the authors; licensee MDPI, Basel, Switzerland. This article is an open access article distributed under the terms and conditions of the Creative Commons Attribution license (<http://creativecommons.org/licenses/by/3.0/>).